ELSEVIER

Journal of Nuclear Materials 249 (1997) 223–230

journal of nuclear materials

Melting behaviour of oxide systems for heterogeneous transmutation of actinides. I. The systems Pu–Al–O and Pu–Mg–O

Hengzhong Zhang [1], M.E. Huntelaar, R.J.M. Konings *, E.H.P. Cordfunke

Netherlands Energy Research Foundation ECN, P.O. Box 1, 1755 ZG Petten, The Netherlands

Received 7 January 1997; accepted 30 May 1997

Abstract

The melting behaviour of the systems $MgO–PuO_{2-x}$ and $Al_2O_3–PuO_{2-x}$ were studied using the CALPHAD method. According to the results of the phase diagram calculations, the temperature at which a liquid starts to form, ranges from 2341 to 2503 K for the system $MgO–PuO_{2-x}$, and from 2049 to 2183 K for the system $Al_2O_3–PuO_{2-x}$, when the oxygen content of PuO_{2-x} changes from 1.61 to 2. © 1997 Elsevier Science B.V.

1. Introduction

Partitioning and transmutation is considered to be a complementary option in the management of the waste from nuclear power generation [1]. In this process the radionuclides are separated from the spent fuel, followed by fission or transmutation in reactors or accelerators. As the long-term radiotoxicity of the fission products is much less than that of the actinides after about 250 years, a substantial reduction of the radiotoxicity of the waste can be achieved.

Plutonium is one of the actinides formed by neutron capture in ^{238}U during irradiation of UO_2 in nuclear power plants. Efficient partitioning of plutonium from the spent fuel has already been realized in present commercial PUREX (plutonium reprocessing and extraction) installations. For the fabrication of fuels for transmutation, two ways are considered: homogeneous mixing in fresh MOX (mixed oxide) fuel, and heterogeneous dispersion in an inert support material. Some oxides, such as aluminium oxide, magnesium oxide and spinel, are appropriate candidate inert matrix materials for heterogeneous transmutation based on an evaluation of some of their physico–chemical and neutronic properties [1–3]. Among these properties the melting behaviour is extremely important. An inert-matrix fuel should have a high melting temperature, preferably above 2273 K to avoid melting of the fuel during power ramps. Consequently, the knowledge of the phase equilibria of fuels consisting of plutonium oxides and inert matrix oxides is of great importance.

There exists only limited thermodynamic information about the systems containing plutonium oxides. This is probably due to the experimental difficulties arising from the relatively high radiotoxicity and chemicotoxicity of plutonium compounds. In some studies, however, cerium has been used as a substitute for plutonium [4,5]. In the present study the CALPHAD technique (computer coupling of phase diagrams and thermochemistry) will be used to calculate the phase equilibria in the systems formed by cerium dioxide, aluminium oxide, magnesium oxide, and plutonium oxides. On the basis of the results obtained, conclusions will be presented with respect to the melting behaviour of the oxide systems $MgO–PuO_{2-x}$ and $Al_2O_3–PuO_{2-x}$.

2. Literature assessment

2.1. $PuO_{1.5}$–PuO_2

The plutonium–oxygen system is a basic system for evaluation of the systems containing plutonium oxides, because the chemical potential of oxygen can influence the

* Corresponding author. Tel.: +31-22 456 4138; fax: +31-22 456 3608; e-mail: konings@ecn.nl.

[1] Visiting scientist on leave from the Department of Chemistry, Central South University of Technology, Changsha, Hunan 410083, People's Republic of China.

PII S0022-3115(97)00182-7

Table 1
Special points in the $PuO_{1.5}$–PuO_2 system

Special points	O/Pu	T (exp.) (K)	T (ass.) (K)	Ref.
M.p. of $PuO_{1.5}$	1.50		2358 ± 25	[9]
	1.50		2353	[10]
Solidus of $PuO_{1.61}$	1.61	2573		[12]
Liquidus of $PuO_{1.62}$	1.62	2553 ± 30		[13]
	1.62	2553 ± 20		[14]
M.p. of PuO_{2-x} ($2-x \rightarrow 1.61$)	1.61	2573		[15,16]
M.p. of $PuO_{1.61}$	1.61		2573 ± 40	present work
M.p. of PuO_2	2.00		2663 ± 40	[9]
	2.00		2698 ± 25	[10]
Eutectic point	1.53		2273	[10]
	1.52		2247	present work [a]
Maximum point in solidus and liquidus lines	1.75	2740		[19]
	1.77		2748	present work [a]

[a] See Section 4.1.1.

phase equilibria. The Pu–O system was reviewed in Refs. [6–10]. The high temperature part of the Pu–O phase diagram in Ref. [10] is shown in Fig. 1 [2]. In the system several phases have been identified: hexagonal (hex) $PuO_{1.5}$, bcc $PuO_{1.52}$, bcc $PuO_{1.61}$ and fcc PuO_{2-x}.

Table 1 lists some special points in the Pu–O system. The bcc $PuO_{1.52}$ phase can only exist below 723 K [10]. The bcc $PuO_{1.61}$ phase can only exist below 1450 K [11] above which it is the stable region of the fcc PuO_{2-x} phase with the homogeneous field of $0 \leq x \leq 0.39$. The fcc phase of $PuO_{1.61}$ is a boundary phase of PuO_{2-x} at the lower limiting oxygen content 1.61. $PuO_{1.61}$ is a nonstoichiometric phase, it has no congruent melting point in principle. Nevertheless it can be reasonably treated as a line compound based on the experimental information in Refs. [12–16] (see Table 1). A value of 2573 ± 40 K can be recommended as the 'melting point' of $PuO_{1.61}$ (also Ref. [17]). The melting points of PuO_2 given in the assessments [9,10] are consistent with each other within the range of uncertainty.

According to Ref. [10] there is a eutectic point between $PuO_{1.5}$ and PuO_{2-x} at 2273 K and O/Pu = 1.53 (60.5 at.% O) by estimation. This eutectic temperature is the mathematical mean of the values 2243 K [20] and 2303 K [14] which was arbitrarily selected. In Ref. [10] the liquidus and solidus lines between PuO_2 and this eutectic point were tentatively drawn as continuously decreasing curves. However, according to available experimental solidus and liquidus data of PuO_{2-x} (see Table 2), there is a maximum at about 2740 K and O/Pu = 1.75 [18,19], which opposes the shapes of the solidus curve and the liquidus curve given in Ref. [10]. The data obtained in Refs. [18,19] were measured by an automatic optical pyrometer, their previous data based on visual observation in Ref. [12] were not selected because of their large scattering. In addition, another two points were found in Ref. [8].

2.2. MgO–CeO_2

The liquidus temperatures of the system MgO–CeO_2 were determined by using an argon plasma jet with an optical pyrometer [21]. In the study X-ray diffraction was used to examine the crystalline phases; the change in the lattice parameter was used to determine the solid solubility of MgO in CeO_2. In the argon plasma, molten CeO_2 was partially reduced to Ce_2O_3. Thus the liquidus data obtained are actually those for the ternary MgO–CeO_2–Ce_2O_3 system. It is assumed that, since CeO_2 was reduced only by a small amount, the determined liquidus temperatures is close to those of the MgO–CeO_2 system. The determined eutectic point of the system is at 2733 ± 50 K and 30 mol% CeO_2.

2.3. MgO–PuO_2

The MgO–PuO_2 system was found to be simply eutectic with limited solid solubility of MgO in PuO_2 [22]. In

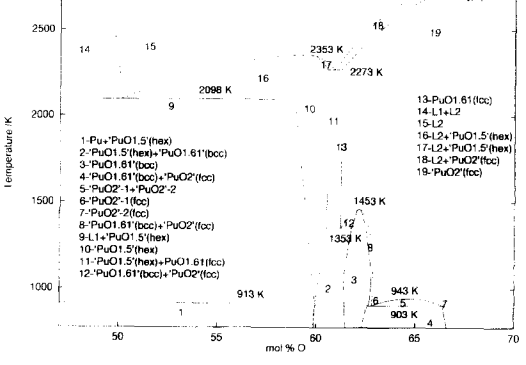

Fig. 1. A part of the Pu–O phase diagram [10].

[2] It should be noted that this figure contains some errors.

Table 2
Liquidus and solidus data for the system $PuO_{1.5}$–PuO_2

Composition, O/Pu	Solidus temp. (K)	Liquidus temp. (K)	Ref.
1.66		2708	[8]
1.68	2678		[8]
1.731	2743	2743	[18,19]
1.785	2740	2745	[18,19]
1.846	2718	2743	[18,19]

the investigation [22], the eutectic point was determined by melting a range of compositions in air, and identifying the primary phases present by metallography. X-ray diffraction and microprobe analyses were used to determine the terminal solid solubility. The oxygen content of plutonium oxide in the samples was confirmed unchanged. The experimental uncertainty of the eutectic temperature 2533 ± 30 K at 40 mol% PuO_2 may be actually larger, because temperatures above 2313 K were extrapolated from calibration curves of the optical pyrometer employed.

2.4. MgO–PuO_{2-x}

The phase diagram of the system MgO–PuO_{2-x} was proposed in Ref. [16] based on photomicrographs of molten specimens of various compositions. It is a simple eutectic one, with the eutectic point at 43 mol% MgO and 2258 ± 35 K. This eutectic temperature was previously reported as 2373 K at the same composition [15]. The difference is probably due to the scattering of the liquidus data obtained in the same investigator's different research courses. It must be pointed out that the eutectic composition was erroneously cited as 43 mol% PuO_2 by several authors [7,23,24]. Since the determination was carried out in a dry helium atmosphere, the starting material PuO_2 was easily reduced to $PuO_{1.61}$ ($2-x=1.61$) (see Refs. [17,22]). Therefore the phase diagrams determined in the works [15,16] are actually for the system MgO–$PuO_{1.61}$.

2.5. Al_2O_3–PuO_2

The phase diagram of the system Al_2O_3–PuO_2 was found to be a simple eutectic one [22]. The eutectic point is at 2183 ± 15 K and 42 mol% PuO_2. Unlike the system MgO–PuO_2, no significant solid solubility was found in this system.

3. Thermodynamic data of pure oxides

In thermodynamic analysis, consistent and reliable thermodynamic data of substances should be selected. At ECN thermodynamic data of a number of nuclear materials were critically assessed and stored in the thermodynamic database, ECN-Tbase [9,25]. Therefore, in the present study the thermodynamic data used for CeO_2, $PuO_{1.5}$, $PuO_{1.61}$(s) and PuO_2 are from ECN-Tbase. The data for the liquid $PuO_{1.61}$ are estimated (see Appendix A). Those used for MgO and Al_2O_3 are from SGTE [26] considering that the essential data for MgO and Al_2O_3 in SGTE and in ECN-Tbase are both based on CODATA, and that the thermodynamic assessment of the system MgO–Al_2O_3 by Hallstedt [26] will be utilized for further study of the ternary system MgO–Al_2O_3–PuO_2. The data for the metastable MgO(fcc) phase are from Ref. [27].

4. Phase diagram calculation

The least-square optimization programs BINGSS and BINFKT [28,29] were used to perform the thermodynamic phase diagram optimization of binary systems. Phase diagrams were then generated using the program MTDATA [30] with the model parameters obtained in the optimization. In ternary phase diagram calculations, the Muggianu method [31] was used.

4.1. Binary systems

4.1.1. $PuO_{1.61}$–PuO_2

Because experimental information of this system is limited (see Section 2.1), $PuO_{1.61}$ and PuO_2 are considered to be line compounds and the $PuO_{1.61}$–PuO_2 system is assumed to be an ideal solid solution (i.e., the fcc PuO_{2-x} phase), considering that $PuO_{1.61}$ and PuO_2 have related crystal structures. A sub-regular solution model can be used to model the liquid phase. From the optimization the solution model parameters can be obtained (Ref. [17]).

The calculated phase diagram is shown in Fig. 2. The calculated maximum point in the liquidus and solidus lines (2748 K and O/Pu = 1.77) is consistent with the literature [19]. Though the two points from Ref. [8] were not used in

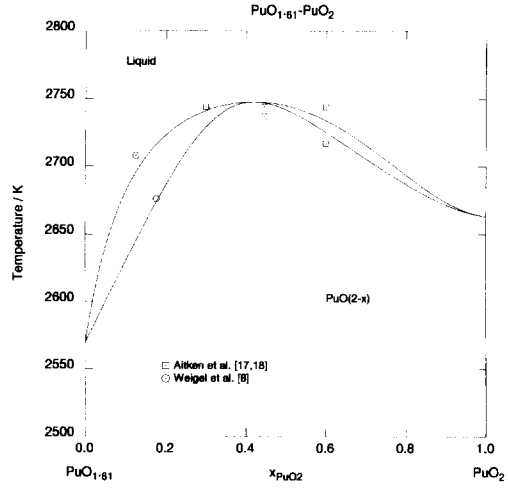

Fig. 2. Calculated phase diagram of the system $PuO_{1.61}$–PuO_2.

the parameter optimization, they are well predicted by the calculation.

4.1.2. MgO–CeO_2

In this system the fcc CeO_2 phase can dissolve a certain amount of MgO and forms a terminal solid solution [21]. It can be modelled as a regular solid solution of MgO(fcc) and CeO_2(fcc).

An association model [32] was chosen to model the liquid phase of the system. The associate $2MgO \cdot CeO_2(l)$ was assumed to form in the liquid phase by trial and error. The solution model parameters, one for the fcc solid solution and four for the liquid phase, can be obtained from the optimization (Ref. [17]). Fig. 3 shows the calculated phase diagram of the system. It can be seen that the calculation fits the experiments fairly well. The point on the left side could not be modelled either with the association model or with a Redlich–Kister polynomial.

4.1.3. MgO–PuO_2

Because there are only one eutectic data point and one solubility data point available for this system [22], only one model parameter for the solid solution and two independent model parameters for the liquid phase can be optimized. In this case the terminal solid solution of the MgO–PuO_2 system was modelled as a regular solution of MgO(fcc) and PuO_2(fcc). The association model [32] was used to model the liquid phase. In order to obtain all four association model parameters from optimization, the liquid association model parameters of the system MgO–CeO_2 were transposed to the system MgO–PuO_2. Considering that CeO_2 is a suitable substitute for PuO_2 [4], the following assumptions were made:

- the interaction parameters between the species in the liquid phase of the MgO–PuO_2 system are proportional to those of the system MgO–CeO_2;
- the difference between the Gibbs energies of formation from the constituent oxides of the two liquid associates, $2MgO \cdot CeO_2$ and $2MgO \cdot PuO_2$, is independent of temperature.

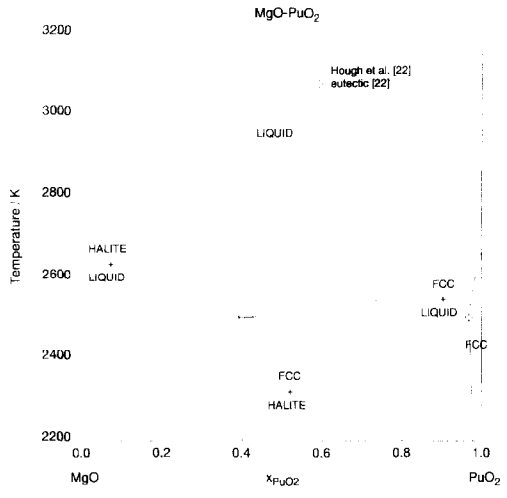

Fig. 4. Calculated phase diagram of the system MgO–PuO_2.

The eutectic temperature $T_{eut} = 2533 \pm 30$ K at 40 mol% PuO_2 [22] was adjusted to $T_{eut} = 2503$ K in order to make the optimization successful. This adjustment is reasonable since the adjusted temperature is still within the experimental error. Solution model parameters were then optimized (Ref. [17]). The calculated phase diagram (Fig. 4) shows that the liquidus curve on the MgO-side decreases steeply with the addition of PuO_2, whereas that on the PuO_2-side decreases gradually with the addition of MgO.

4.1.4. MgO–$PuO_{1.61}$

The MgO–$PuO_{1.61}$ system is a simple eutectic one (see Section 2.4). The liquid phase of the system can be modelled as a sub-regular solution model (Ref. [17]). Fig. 5 is the calculated phase diagram of the system. The calculated eutectic composition, 54 mol% $PuO_{1.61}$, is close

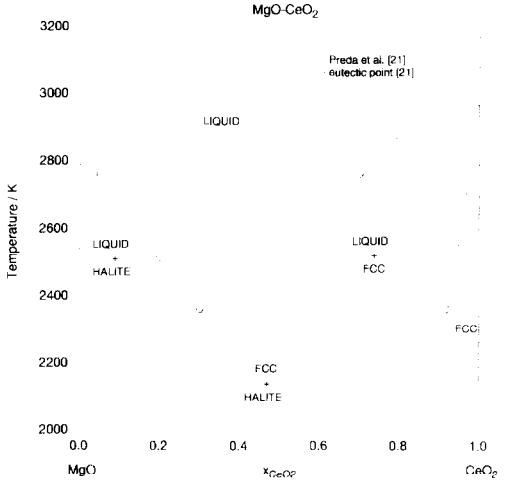

Fig. 3. Calculated phase diagram of the system MgO–CeO_2.

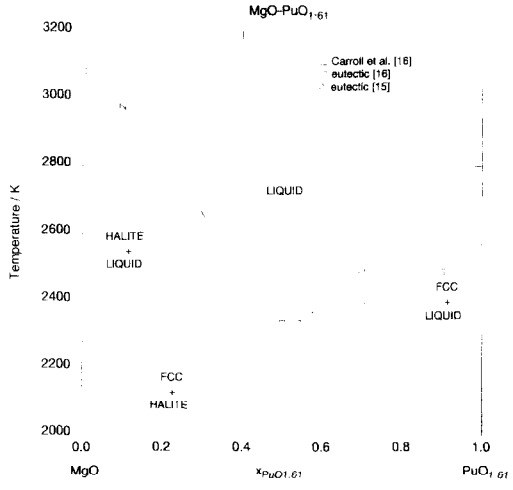

Fig. 5. Calculated phase diagram of the system MgO–$PuO_{1.61}$.

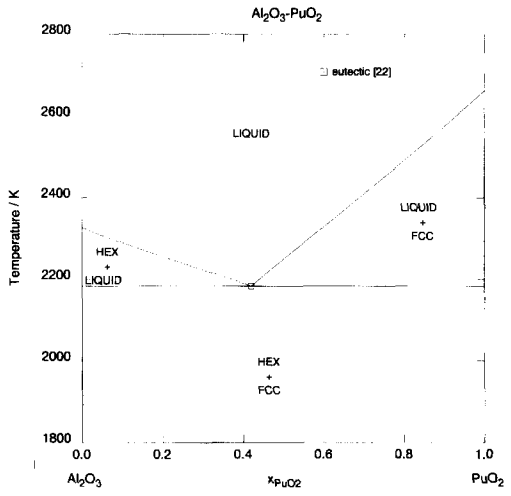

Fig. 6. Calculated phase diagram of the system Al_2O_3–PuO_2.

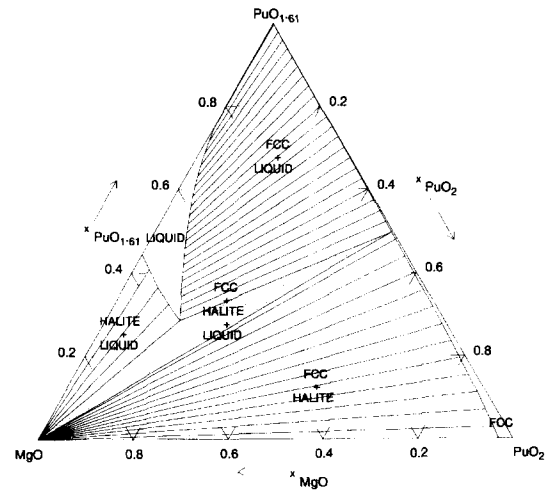

Fig. 7. Calculated isothermal section of the MgO–$PuO_{1.61}$–PuO_2 system at 2450 K.

to the 57 mol% given in Ref. [16]. The calculated eutectic temperature 2341 K is between the values of 2258 K [16] and 2373 K [15].

4.1.5. Al_2O_3–PuO_2

According to Ref. [22], the Al_2O_3–PuO_2 system is a simple eutectic one. The liquid phase can be modelled with a sub-regular solution model (Ref. [17]). The calculated phase diagram is shown in Fig. 6.

4.1.6. Al_2O_3–$PuO_{1.61}$

No experimental information about the phase equilibria in this system is available. It is assumed that the Al_2O_3–$PuO_{1.61}$ system is simply eutectic like the Al_2O_3–PuO_2 one, and that the liquid phase behaves ideally. With this assumption, the eutectic point was calculated to be at 2049 K and 52 mol% $PuO_{1.61}$.

4.1.7. Summary of eutectic points

The eutectic points of the above binary systems are summarized in Table 3 which shows that the calculated values are consistent with the experimental values.

Table 3
Summary of the eutectic points

System (1)–(2)	mol% (2)		T (calc.) (K)	T (expt.) (K)	Ref.
	calc.	expt.			
MgO–CeO_2	30	30	2362	2373 ± 50	[21]
MgO–PuO_2	40	40	2503	2533 ± 30	[22]
MgO–$PuO_{1.61}$	54	57	2341	2258 ± 35	[16]
	54	57	2341	2373	[15]
Al_2O_3–PuO_2	42	42	2183	2183 ± 15	[22]
Al_2O_3–$PuO_{1.61}$	52		2049		

4.2. Ternary systems

4.2.1. MgO–$PuO_{1.61}$–PuO_2

The isothermal sections of the MgO–$PuO_{1.61}$–PuO_2 system were calculated from 2200 to 3100 K. According to the calculations, liquid is present in some phase fields of the system above 2341 K. The calculated isothermal phase diagram at 2450 K (Fig. 7) shows that when the mole ratio of PuO_2 to $PuO_{1.61}$ is less than $0.5/0.5 = 1.0$, or the oxygen content of PuO_{2-x} is less than 1.81, a liquid starts to form from the fcc + halite mixture. Fig. 8 shows a temperature vs. composition section in the ternary phase diagram (isopleth T–x diagram) of the pseudo-binary system MgO–$PuO_{1.81}$. It can be seen from Fig. 8 that in the pseudo-binary system a liquid starts to form from the fcc + halite mixture when the temperature reaches 2450 K.

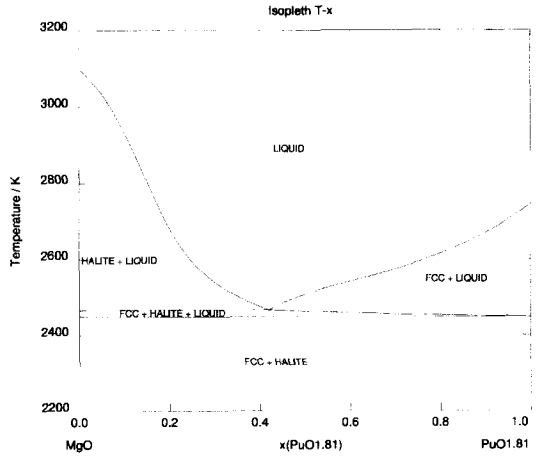

Fig. 8. Isopleth $T-x$ diagram of the pseudo-binary MgO–$PuO_{1.81}$ system.

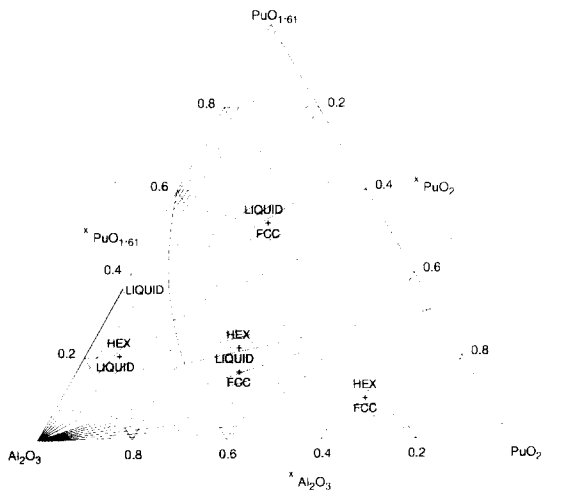

Fig. 9. Calculated isothermal section of the Al_2O_3–$PuO_{1.61}$–PuO_2 system at 2150 K.

Thus, in order to avoid the occurrence of a liquid, the oxygen content of PuO_{2-x} should be higher than 1.81 at 2450 K, or the temperature should be lower than 2450 K at the oxygen content 1.81.

4.2.2. Al_2O_3–$PuO_{1.61}$–PuO_2

The isothermal sections of the Al_2O_3–$PuO_{1.61}$–PuO_2 system were calculated from 2000 to 2450 K. According to the calculations, liquid is present in some phase fields of the system at temperatures above 2049 K. Fig. 9 shows the calculated phase diagram at 2150 K. According to Fig. 9, at 2150 K the mole ratio of PuO_2 to $PuO_{1.61}$ should be greater than $0.67/0.33 = 2.0$, or the oxygen content of PuO_{2-x} should be greater than 1.87 in order to prevent the occurrence of liquid. Fig. 10 shows the isopleth T–x diagram of the Al_2O_3–$PuO_{1.87}$ pseudo-binary system, according to which the temperature should be lower than

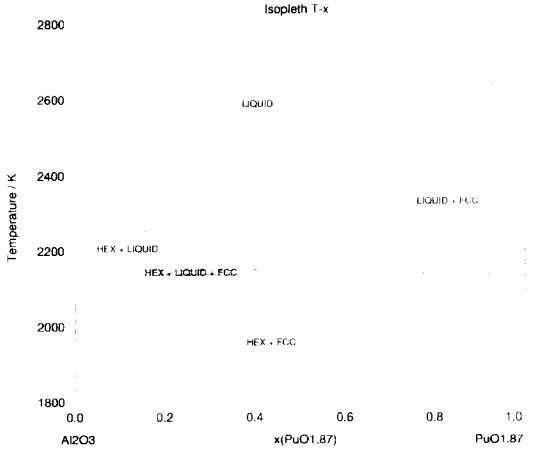

Fig. 10. Isopleth $T-x$ diagram of the pseudo-binary Al_2O_3–$PuO_{1.87}$ system.

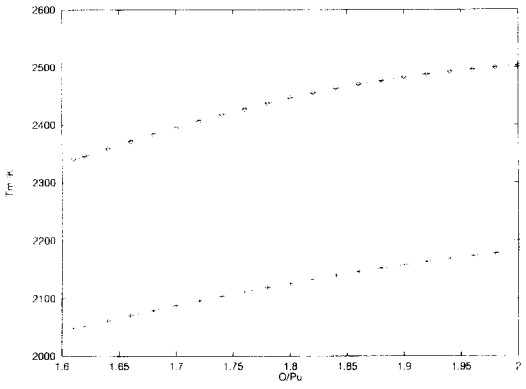

Fig. 11. Variation of 'melting temperature' with the oxygen content of plutonium oxide (diamond: MgO–PuO_{2-x}; plus: Al_2O_3–PuO_{2-x}).

2150 K in order to prevent the occurrence of liquid at the oxygen content 1.87.

5. Discussion and conclusion

From the isopleth T–x diagram calculations of the ternary systems MgO–$PuO_{1.61}$–PuO_2 and Al_2O_3–$PuO_{1.61}$–PuO_2, the temperatures at which a liquid starts to form in the systems MgO–PuO_{2-x} and Al_2O_3–PuO_{2-x} can be obtained, as shown in Fig. 11. This temperature is referred to as the 'melting temperature' of the system hereafter.

At thermodynamic equilibrium, the oxygen content of PuO_{2-x} is determined by the oxygen potential at that temperature. Using the assessments of the oxygen potential of PuO_{2-x} given in Refs. [33,34], the oxygen potential at a certain temperature and a certain oxygen content can be calculated. It was proved according to these calculations that the equilibrium oxygen pressure of PuO_{2-x} is much higher than the dissociation pressure of MgO (or Al_2O_3), thus the oxygen potential over a MgO + PuO_{2-x} mixture

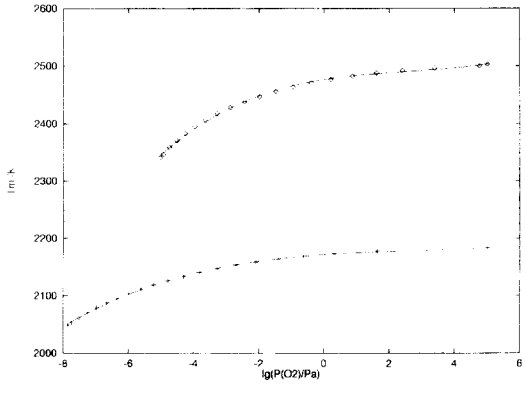

Fig. 12. 'Melting temperatures' as a function of the P/Pu ratio in the systems MgO–PuO_{2-x} (diamond) and Al_2O_3–PuO_{2-x}) (plus).

(or an $Al_2O_3 + PuO_{2-x}$ mixture) is actually dominated by the oxygen potential of PuO_{2-x}. As a result, we can calculate the variation of the 'melting temperature' with the oxygen potential, as shown in Fig. 12.

The following regression equations can represent the curves in Figs. 11 and 12 very well. For the system $MgO–PuO_{2-x}$:

$$T_m/K = -688 + 3053(O/Pu) - 729(O/Pu)^2 \quad (1.61 \le (O/Pu) \le 2), \tag{1}$$

$$T_m/K = 2477 + 8.87\log(p(O_2)/Pa) - 2.06[\log(p(O_2)/Pa)]^2 + 0.27[\log(p(O_2)/Pa)]^3 \quad (-5.03 \le \log(p(O_2)/Pa) \le 5.01); \tag{2}$$

and for the system $Al_2O_3–PuO_{2-x}$:

$$T_m/K = 440 + 1524(O/Pu) - 326(O/Pu)^2 \quad (1.61 \le (O/Pu) \le 2), \tag{3}$$

$$T_m/K = 2172 + 3.77\log(p(O_2)/Pa) - 0.74[\log(p(O_2)/Pa)]^2 + 0.093[\log(p(O_2)/Pa)]^3 \quad (-7.86 \le \log(p(O_2)/Pa) \le 5.01). \tag{4}$$

Fig. 11 shows that the 'melting temperature' increases with the oxygen content of plutonium oxide. Below the 'melting temperature' the matrix oxide coexists with plutonium oxide, above this temperature the solids melt. The 'melting temperature' of the $MgO–PuO_{2-x}$ system is higher than that of the $Al_2O_3–PuO_{2-x}$ system by 280 to 320 K when O/Pu changes from 1.61 to 2. Fig. 12 shows that the 'melting temperature' increases strongly with the oxygen potential at first, but when the oxygen pressure reaches about 1 Pa, the increase of the 'melting temperature' levels off. In the process of heterogeneous transmutation of plutonium, the temperature of the fuel increases due to the decrease of the thermal conductivity resulting from the accumulation of fission products and radiation damage. As long as the temperature remains below the values given by the 'melting temperature' curve in Figs. 11 and 12, liquid formation is avoided. Consequently it is expected that melting does not occur when the temperature of the fuel remains below the values given in Eqs. (1) and (2) for the $MgO–PuO_{2-x}$ system, and the values given in Eqs. (3) and (4) for the $Al_2O_3–PuO_{2-x}$ system.

Appendix A. Estimation of melting properties of $PuO_{1.61}$

A.1. $\Delta_{fus}H^0$ and $\Delta_{fus}S^0$

It was suggested in the literature [22,35] that the entropy of fusion per molecule is R (gas constant) per atom, thus

$$\Delta_{fus}H^0/RT_m = \text{number of atoms per molecule.} \tag{A.1}$$

Table 4
Melting properties of plutonium oxides

Oxide	$PuO_{1.5}$	PuO_2
Number of atoms	2.5	3
T_m (K)	2358 ± 25	2663 ± 40
$\Delta_{fus}H^0$ (kJ mol^{-1})	56.5 ± 20	67 ± 15
$\Delta_{fus}H^0/RT_m$	2.882	3.026
Ref.	[9]	[9]

However, as can be seen from Table 4 this equation is not precisely valid, especially for $PuO_{1.5}$. Therefore, a linear interpolation between the values of $\Delta_{fus}H^0/RT_m$ of PuO_2 and $PuO_{1.5}$ is used to estimate that of $PuO_{1.61}$,

$$\Delta_{fus}H^0/RT_m = 2.882 + (3.026 - 2.882) \times (1.61 - 1.5)/(2 - 1.5) = 2.914, \tag{A.2}$$

which results in

$$\Delta_{fus}H^0 = 2.914RT_m = 2.914 \times 8.314 \times 2573 = 62336 \text{ J mol}^{-1}. \tag{A.3}$$

Considering the errors in $\Delta_{fus}H^0$ of PuO_2 and $PuO_{1.5}$ [9], we take the value of $\Delta_{fus}H^0 = 62 \pm 20$ kJ mol^{-1} which results in $\Delta_{fus}S^0 = 24.1 \pm 8.0$ J K^{-1} mol^{-1}.

A.2. $C_p^0(PuO_{1.61}(l))$

It is assumed that the difference between the heat capacities of liquid PuO_2 and liquid $PuO_{1.61}$ is equal to that between the heat capacities of solid PuO_2 and solid $PuO_{1.61}$ at the melting point of $PuO_{1.61}$,

$$C_p^0[PuO_2(l)] - C_p^0[PuO_{1.61}(l)] = C_p^0[PuO_2(s)] - C_p^0[PuO_{1.61}(s)]. \tag{A.4}$$

The value for $C_p^0[PuO_2(s)] - C_p^0[PuO_{1.61}(s)]$ at the melting point of $PuO_{1.61}$ (2573 K) is calculated to be 6.14 J K^{-1} mol^{-1} using the thermodynamic data in ECN-Tbase [9]. Therefore,

$$C_p^0[PuO_{1.61}(l)] = C_p^0[PuO_2(l)] - 6.14 = 131 - 6.14 \simeq 125 \text{ J K}^{-1} \text{ mol}^{-1}, \tag{A.5}$$

where $C_p^0[PuO_2(l)] = 131$ J K^{-1} mol^{-1} is also taken from ECN-Tbase [9].

References

[1] L.H. Baetslé, IAEA Bull. 3-1992 (1992) 32.
[2] N. Cocuaud, T. Duverneix, R. Mazoyer, Y. Philipponneau, J.M. Adnet, J.P. Dancausse, in: Proc. Global '95, Int. Conf. on Evaluation of Emerging Nuclear Fuel Cycle Systems, Versailles, France, Sept. 11–14, 1995, p. 530.
[3] C. Prunier, Y. Guerin, J. Faugere, N. Cocuaud, J.M. Adnet, in: Proc. Global '95, Int. Conf. on Evaluation of Emerging Nuclear Fuel Cycle Systems, Versailles, France, Sept. 11–14, 1995, p. 506.

[4] J.M. Haschke, in: Transuranium Elements: A Half Century, eds. L.R. Morss and J. Fuger (American Chemical Society, Washington, DC, 1992) p. 416.
[5] A.G. Raraz, B. Mishra, D.L. Olson, J.J. Moore, AC3490DP62349, 1992.
[6] D.T. Livey, P. Feschotte II, Atom. Energy Rev. 4 (1) (1966) 53, special issue.
[7] International Atomic Energy Agency, The Plutonium–Oxygen and Uranium–Plutonium–Oxygen Systems: A Thermochemical Assessment, Techn. Rep. Ser. No. 79, Vienna, 1967.
[8] F. Weigel, J.J. Katz, G.T. Seaborg, Plutonium, in: The Chemistry of the Actinide Elements, eds. J.J. Katz, G.T. Seaborg and L.R. Morss, Vol. 1 (Chapman and Hall, London, 1986) p. 499.
[9] E.H.P. Cordfunke, R.J.M. Konings, Thermochemical Data for Reactor Materials and Fission Products (North-Holland, Amsterdam 1990).
[10] H.A. Wriedt, Bull. Alloy Phase Diagrams 11 (1990) 184.
[11] T.M. Besmann, J. Nucl. Mater. 144 (1987) 141.
[12] E.A. Aitken, S.K. Evans, A Thermodynamic Data Program Involving Plutonia and Urania at High Temperatures, Nucleonics Laboratory Quart. Rep. No. 2, GEAP-5395, 1968.
[13] T.D. Chikalla, J. Am. Ceram. Soc. 46 (1963) 324.
[14] T.D. Chikalla, C.E. McNeilly, R.E. Ksavdahl, J. Nucl. Mater. 12 (1964) 131.
[15] D.F. Carroll, in: Hanford Laboratories Report, HW-76303, 1963, p. 2.1.
[16] D.F. Carroll, J. Am. Ceram. Soc. 47 (1964) 650.
[17] H. Zhang, M.E. Huntelaar, R.J.M. Konings, E.H.P. Cordfunke, Melting Behaviour of Oxide Systems for Heterogeneous Transmutation of Actinides, Netherlands Energy Research Foundation ECN, Report ECN-I-96-046, 1996.
[18] E.A. Aitken, S.K. Evans, A Thermodynamic Data Program Involving Plutonia and Urania at High temperatures, Nucleonics Laboratory Quart. Rep. No. 3, GEAP-5634, 1968.
[19] E.A. Aitken, S.K. Evans, A Thermodynamic Data Program Involving Plutonia and Urania at High temperatures, Nucleonics Laboratory Quart. Rep. No. 4, GEAP-5672, 1968.
[20] B. Riley, Sci. Ceram. 5 (1970) 83.
[21] M. Preda, R. Dinescu, Rev. Roum. Chim. 21 (1976) 1023.
[22] A. Hough, J.A.C. Marples, J. Nucl. Mater. 15 (1965) 298.
[23] S. Casalta, K. Richter, C. Prinier, In: Proc. Global '95, Int. Conf. on Evaluation of Emerging Nuclear Fuel Cycle Systems, Sept. 11–14, 1995, Versailles France, p. 1725.
[24] Institute for Transuranium Elements, Annual Report EUR 16368, 1995, p. 111.
[25] E.H.P. Cordfunke, R.J.M. Konings, J. Phase Equilib. 14 (1993) 457.
[26] B. Hallstedt, J. Am. Ceram. Soc. 75 (1992) 1497.
[27] E.H.P. Cordfunke, M.E. Huntelaar, M.A. Mignanelli, 3th Frame Work Programme of the European Union, 1996, to be published.
[28] H.L. Lukas, S.G. Fries, J. Phase Equilib. 13 (1992) 532.
[29] H.L. Lukas, S. Fries, U. Kattner, J. Weiss, BINGSS, BINFKT, TERGSS and TERFKT Reference Manual, Version 95–1, 1995.
[30] AEA Technology, MTDATA Handbook, 1994.
[31] M. Hillert, Calphad 4 (1980) 1.
[32] F. Sommer, Z. Metallkd. 73 (1982) 72.
[33] T. Besmann, B. Lindemer, J. Nucl. Mater. 130 (1985) 489.
[34] T. Besmann, B. Lindemer, J. Nucl. Mater. 137 (1986) 292.
[35] L.F. Epstein, W.H. Howland, J. Am. Ceram. Soc. 36 (1953) 334.